VOLUME 116, NUMBER 16
AUGUST 10, 1994

JOURNAL
OF THE
AMERICAN
CHEMICAL
SOCIETY

A New DNA Minor Groove Binding Motif: Cross-Linked Lexitropsins

Yong-Huang Chen and J. William Lown*

Contribution from the Department of Chemistry, University of Alberta, Edmonton, Alberta, Canada T6G 2G2

Received November 18, 1993®

Abstract: The nitrogen atoms of central pyrrole rings on two separate tripyrrolecarboxamide strands were covalently linked through poly(methylene) chains to provide a novel class of lexitropsins potentially capable of B-DNA double-strand reading via the minor groove. CD titration experiments revealed increasingly enhanced binding of 1:1 stoichiometry to the poly(dA-dT)-poly(dA-dT) DNA from the tetrakis(methylene) linkage to the heptakis(methylene) linkage, suggesting gradually growing importance of the bidentate antiparallel side by side binding. Ethidium bromide fluorescence displacement experiments on both poly(dA-dT)-poly(dA-dT) and poly(dA)-poly(dT) DNA's supported this analysis by providing quantitative measurement of intrinsic binding constants. The heptakis(methylene) linkage offered a binding enhancement of approximately 1000 times compared with that of the monomer.

Recent studies on DNA-binding mechanisms of netropsin, distamycin, and their generalized information-reading analogues, the so-called "lexitropsins", have revealed a new structural motif different from what was previously observed from X-ray diffraction analysis on crystals of these minor grove binders and oligonucleotides.[1] Two identical or different peptidic lexitropsins packing in the minor groove in an antiparallel side by side manner with each positively charged end pointing outward to the 3′ end of its neighboring DNA strand (i.e., WPPW-*apss*-o-(3′,3′)),[1c] constitute this structural unit, as illustrated in Scheme 1. Although this model was proposed earlier by Zimmer et al.,[2] the definitive proof and structural details were not available until

Scheme 1. The WPPW Binding Motif

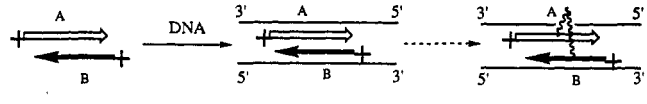

Wemmer et al.[3] carried out NMR studies on binding interactions between distamycin and several oligonucleotides. Studies on imidazole and pyridine containing lexitropsins by Dervan's[4] and Lown's[5] groups provided a broadened picture of this new binding motif. Much higher cooperativity was observed for binding of these lexitropsins to GC-containing base sequences. More

* Author to whom correspondence should be addressed.
® Abstract published in *Advance ACS Abstracts,* July 1, 1994.

(1) (a) Kopka, M. L.; Yoon, C.; Goodsell, D.; Pjura, P.; Dickerson, R. E. *J.Mol. Biol.* **1985**, *183*, 553–563. (b) Coll, M.; Frederick, C. A.; Wang, A. H.-J.; Rich, A. *Proc. Natl. Acad. Sci. U.S.A.* **1987**, *84*, 8385–8389. (c) For the sake of clarity, binding motif and stoichiometry must be differentiated. WPW, WPPW, and *WPPW* stand for the groove wall–peptide–groove wall motif, the groove wall–peptide–peptide–groove wall motif, and the covalently linked groove wall–peptide–peptide–groove wall motif, respectively. *apss*-o-(3′,3′) further specifies the antiparallel side by side arrangement with two positively charged ends located outside and pointing to the 3′ direction of the corresponding adjacent strand.

(2) (a) Luck, G.; Zimmer, C.; Reinert, K. E.; Atcamone, F. *Nucleic Acids Res.* **1977**, *4* (8), 2655–2670. (b) Reinert, R. E. *Biophys. Chem.* **1981**, *13*, 1–14. (c) Burckhardt, G.; Votavova, H.; Sponar, J.; Luck, G.; Zimmer, C. *J. Biomol. Struct. Dyn.* **1985**, *2* (4), 721–736.

(3) (a) Pelton, J. G.; Wemmer, D. E. *Proc. Natl. Acad. Sci. U.S.A.* **1989**, *86*, 5723–5727. (b) Pelton, J. G.; Wemmer, D. E. *J. Am. Chem. Soc.* **1990**, *112*, 1393–1399. (c) Fagan, P.; Wemmer, D. E. *J. Am. Chem. Soc.* **1992**, *114*, 1080–81.

(4) (a) Wade, W. S.; Dervan, P. B. *J. Am. Chem. Soc.* **1987**, *109*, 1574–1575. (b) Wade, W. S.; Mrksich, M.; Dervan, P. B. *J. Am. Chem. Soc.* **1992**, *114*, 8783–8792. (c) Mrksich, M.; Wade, W. S.; Dwyer, T. J.; Geierstanger, B. H.; Wemmer, D. E.; Dervan, P. B. *Proc. Natl. Acad. Sci. U.S.A.* **1992**, *89*, 7586–7590. (d) Mrksich, M.; Dervan, P. B. *J. Am. Chem. Soc.* **1993**, *115*, 2572–2576.

0002-7863/94/1516-6995$04.50/0

interestingly, both groups showed that the heterodimeric motif has greater binding strength than the homodimeric one.[4d,5b] Each binding molecule interacts specifically with only one DNA strand, which constitutes a unique strand specific information reading pattern. Overall, the dimeric binding motif (WPPW) opens up possibilities of the minor groove information readout, since structurally controllable variables are now doubled.

Design Rationale

Although the strand specific heterodimeric binding is of high cooperativity and greater binding strength, it does have several disadvantages. First of all, each monomer A or B may act by itself alone through a WPW 1:1 mode. Secondly, the homodimeric binding may compete through a WPPW 2:1 mechanism (AA and BB). These competing mechanisms most likely have different base-sequence specificities. Therefore, the desired base-sequence specific recognition, whether or not the lexitropsins are carriers of DNA reactive functional groups, is difficult to achieve.

One possible solution to this problem is to connect more monomeric binding units covalently while maintaining the same WPPW binding motif. The actual binding mode for the linked molecules may become bidentate binding with a stoichiometry of 1:1.[5c] If an ideal linkage is found, the optimal binding strength K of a covalently linked lexitropsin is more than the product of two stepwise binding constants (k_A and k_B).[6,11d] K is therefore much larger than either binding constant, and the WPW mechanism of 1:1 stoichiometry (i.e., monodentate) is drastically suppressed. The dimeric binding (either homo- or hetero-) is a termolecular process which has an inherent entropy disadvantage compared with that of the bimolecular bidentate binding. When the covalently linked WPPW bidentate binding becomes dominant, the dimeric binding of 2:1 stoichiometry has to compete mainly with the bidentate binding instead of the monodentate binding. The dimeric binding is thus greatly disfavored.

Interestingly, bidentate binding through covalent linkage may allow inherently higher sequence recognition specificity (i.e., resolution) of the WPPW motif to be expressed. Define a single-point resolution (R) of a ligand as the ratio of binding constants before and after a base pair "mutation", e.g., K and K'. Therefore, a dimeric ligand of the *WPPW* motif composed of binding moieties A and B has a resolution $R = K/K' = (k_A k_B)/(k'_A k'_B) \approx R_A R_B$. Here, R_A and R_B represent resolution values for binding moieties A and B, respectively, before they are covalently linked. For poly(pyrrolecarboxamide) ligands in the WPW mode, their single-point resolution values are approximately 10 for the AT to GC "mutation".[16] Therefore, a bidentate ligand composed of two such binding moieties may have a single-point resolution (AT to GC) value of $\sim$100.

End to end covalent linkage of small lexitropsin fragments has been previously employed to increase the length of recognized base sequences and to overcome the phasing problem.[7] But, it is unsuitable for the present problem because two binding fragments have to make a U turn to form a *WPPW* motif, which usually does not happen from footprinting studies of these linked molecules. Enforced rigidity of the end to end linkage to constrain two binding fragments to one side would quite likely cause disturbance of the local DNA structure, as revealed from model inspection. Two simple and distinct means of connecting two fragments, capable of preventing formation of linear binding structures, are envisaged. One is to connect two fragments end to end twice, forming a macrocyclic molecule. The other alternative is to connect nitrogen atoms of two central pyrrole rings once, forming an H-shaped molecule. Scheme 2 illustrates these ideas. One may easily envisage repetition of the latter cross-linkage or combination of the end to end linkage and cross-linkage, generating more complex macrocyclic or ladderlike structures. As is known, the hydrophobic convex edge of bound lexitropsins faces away from the hydrogen-binding region toward the aqueous solution and thus the suitable linkage of pyrrole *N*-methyl groups should not appreciably disturb the total binding interaction. The cross-linked H-shaped molecule is structurally simple, and a single linkage should introduce the least structural disturbance of two binding moieties. We therefore decided to pursue this design first.

Scheme 2. Linkage of Two Lexitropsin Fragments

Double End to End Bis-linkage:

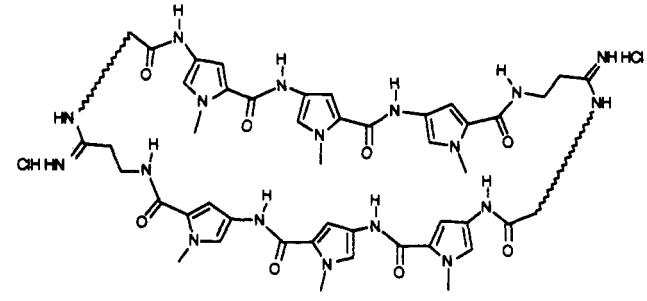

Central Cross Linkage:

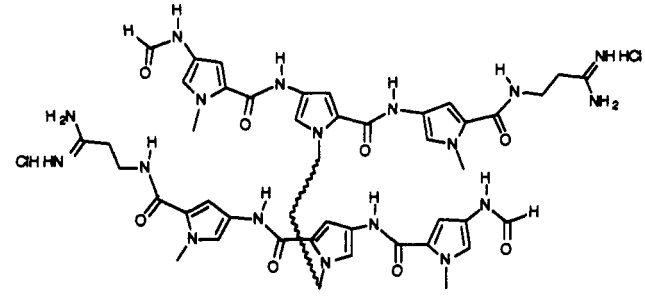

Although an ideal rigid cross-linker may make two fragments more predisposed to effective binding, a less than ideal rigid linker may cause very poor binding because its rigidity makes self-correction to moderately good fitting very difficult. In other words, a rigid linker tends to give an all or nothing situation. In contrast, a flexible linker may scan a larger conformational space and some moderately good fitting is more likely to happen. However, an entropy penalty has to be paid and greater conformational possibilities may create difficulties in binding analysis. Therefore, we selected some short flexible poly(methylene) linkers initially for testing the cross-linkage design. These linkers should also be relatively stable *in vivo*, which is a necessary consideration if the cross-linked lexitropsins are to be used ultimately as carriers for DNA reactive functional groups *in vivo*.

Close inspection of all well-characterized antiparallel side by side (3′,3′) binding structures from NOESY experiments reveals

(5) (a) Dwyer, T.; Geierstanger, B. H.; Bathini, Y.; Lown, J. W.; Wemmer, D. E. *J. Am. Chem. Soc.* **1992**, *114*, 5911–5919. (b) Geierstanger, B. H.; Dwyer, T.; Bathini, Y.; Lown, J. W.; Wemmer, D. E. *J. Am. Chem. Soc.* **1993**, *115*, 4474–4482. (c) A similar idea was expressed in the recent article from Dervan's group, see ref 4d. Shortly after we submitted our manuscript to this journal, two articles regarding studies on a similar series of cross-linked lexitropsins from the Dervan/Wemmer group came to our attention (*J. Am. Chem. Soc.* **1993**, *115*, 9892–9906.). Major conclusions about effects of the aliphatic linker length on binding mode and binding strength from two independent studies are well in conflict with each other. However, the two studies employed very different lexitropsin–DNA interacting systems and binding characterization methodologies.

(6) Chipman, D. M.; Sharon, M. *Science* **1969**, *165*, 454.

(7) (a) Gursky, G. V.; Zasedatelev, A. S.; Zhuze, A. L.; Khorlin, A. A.; Grokhovsky, S. L.; Streltssov, S. A.; Surovaya, A. N.; Nikitin, S. M.; Krylov, A. S.; Retchinsky, V. O.; Mikhailov, M. V.; Beabeallashvili, R. S.; Gottikh, B. P. *Cold Spring Harbor Symp. Quant. Biol.* **1983**, *47*, 367–378. (b) Dervan, P. B. *Science* **1986**, *232*, 464–471. (c) Lown, J. W. *Anti-Cancer Drug Des.* **1988**, *3*, 25–40. (d) Change of the amidinium terminus to dimethylammonium may reduce the overall binding strength but does not appear to have effects on the binding mode. For examples, see: (a) He, G.-X.; Browne, K. A.; Groppe, J. C.; Blasko, A.; Mei, H.-Y.; and Bruice, T. C. *J. Am. Chem. Soc.* **1993**, *115*, 7061–7071. (b) Taylor, J. S.; Schultz, Dervan, P. B. *Tetrahedron* **1984**, *40* (3), 457–465.

Scheme 3. Maximal End to End Distances (Å) of Poly(methylene) Chains

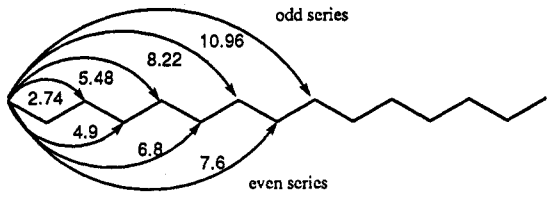

Scheme 4[a]

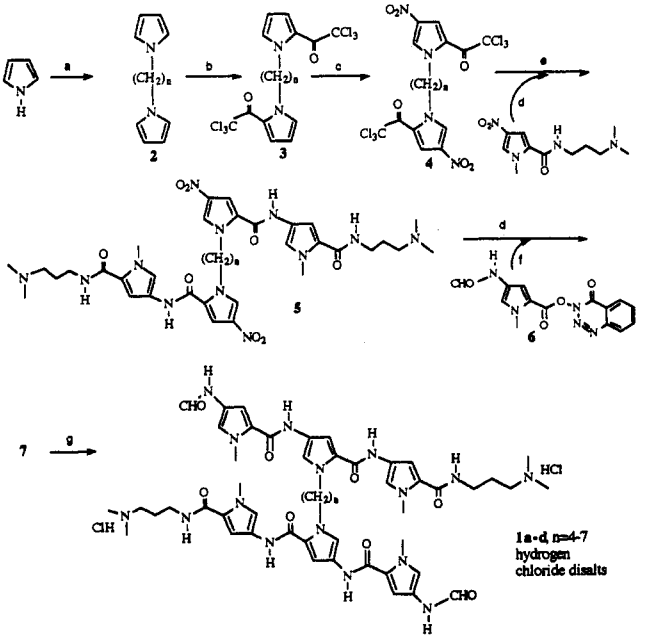

[a] (a) K, THF, reflux; $Br(CH_2)_nBr$, 50–90%. (b) CCl_3COCl, CH_2Cl_2, rt, 85%. (c) Ac_2O, HNO_3, –40 °C to rt, CH_2Cl_2, 45%. (d) H_2, PtO_2, MeOh, rt. (e) DMF, rt, 60%. (f) DMF, 55 °C, 50%. (g) HCl (aq), pH = 5.

the most common arrangement.[3-5] Two separate tricyclic lexitropsins are staggered in such a way that five base pairs are covered, and the distance between *N*-methyl groups of the two central heterocyclic rings (either pyrrole or imidazole) is shortest in comparison with any other arrangement in large part due to the right-handed B-DNA structure. The distance between two central *N*-methyl groups should be not less than the closest distance between two completely overlapping pyrrole rings, which is 3.4 Å, twice the van der Waals radius of sp^2 carbon atoms. Maximal end to end distances of poly(methylene) chains, calculated from a C–C bond length of 1.54 Å and a C–C–C bond angle of 109° 28′, are shown in Scheme 3. The tetrakis(methylene) chain is the shortest possible to meet the geometric requirement just mentioned and was chosen as the starting point of this project.

Synthesis

The first generation of cross-linked target molecules was selected as symmetric ones with dimethylamino termini to simplify the synthetic component.[7d] Once the design concept is validated, the range of molecules can then be expanded. These prototype molecules **1a–d** are shown in Scheme 4. Synthetic design takes the advantage of the symmetry of these molecules.

Pyrrole was converted to its potassium salt by refluxing with potassium in THF. To the generated suspension was introduced the appropriate 1,*n*-dibromoalkane, and the crude product was fractionally distilled to provide the 1,1′-(1,*n*-alkanediyl)bis(pyrrole) **2**.[8] The 1,1′-bis(pyrrole) was then trichloroacetylated

(8) 1,1′-(1,4-Butanediyl)bis(pyrrole) is known: Hodgkin, J. H.; Solomon, D. H. *J. Macromol. Sci., Chem.* **1976**, *A10* (5), 893–992.

Scheme 5[a]

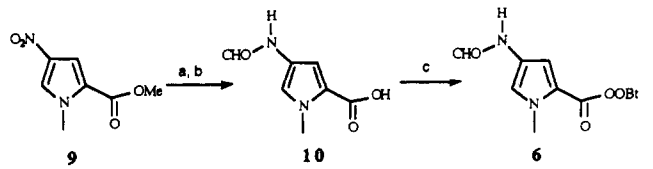

[a] (a) H_2, 10% Pd–C, rt, quantitative. (b) NaOH (aq), rt; HCOOAc, 0 °C, 71%. (c) EDCI, HOOBt, DMF, rt, 67%.

to afford compound **3** in ~85% yield.[9] This intermediate was nitrated with fuming nitric acid in acetic anhydride to 4,4′-dinitro-2,2′-(trichloroacetyl)-1,1′-(1,*n*-alkanediyl)bis(pyrrole) **4** in ~45% yield. The major by-product is the 4,5′-dinitro compound. The coupling reaction of **4** with a freshly prepared *N*-[(dimethylamino)propyl]-1-methyl-4-nitropyrrole-2-carboxamide went smoothly, and the tetrapyrrole intermediate **5** was isolated in ~60% yield. Catalytic hydrogenation with platinum oxide led to an unstable diaminotetrapyrrole intermediate which was applied to the next step without purification. The coupling reaction with activated ester **6** was performed at 50 °C in DMF, producing the neutral hexapyrrole intermediate **7** in ~50%. This compound was acidified to pH = 5 at low temperature. Concentration gave the crude solid which was dissolved in methanol and precipitated with ether to generate hydrochloride disalt **1**. Other electrophiles such as 1-methyl-2-trichloroacetylimidazole and 1-methyl-4-nitro-2-trichloroacetylpyrrole also coupled smoothly with the diaminotetrapyrrole intermediate. The coupling reaction with activated ester **6** was applied to synthesis of monomer **8** from the known precursor *N*-[(dimethylamino)propyl]-1-methyl-4-(1-methyl-4-nitropyrrole-2-carboxamido)pyrrole-2-carboxamide.[9b]

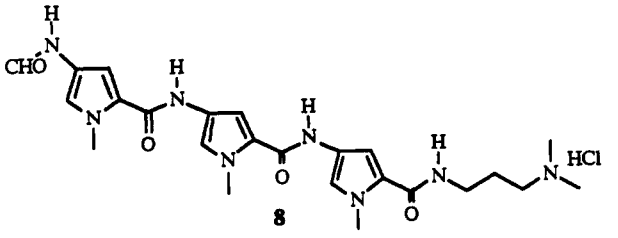

The procedure used to prepare activated ester **6** is shown in Scheme 5. Acid **10** was first prepared from ester **9** by using a procedure different from what was previously reported.[10] Coupling with HOOBt went smoothly with EDCI as the coupling reagent.

Binding Analysis

Construction of the Binding Model. For cross-linked lexitropsins, three binding modes are available when interacting with a DNA duplex possessing a single binding site: the 1:1 stoichiometry modes including the monodentate WPW and the bidentate WPPW modes and the 2:1 stoichiometry WPPW mode, as depicted in Scheme 6. Because

$$k_1 = \frac{[b]}{[DNA][a]}, \quad k_2 = \frac{[c]}{[DNA][a]} \quad \text{and}$$

$$k_4 = \frac{[d]}{[a][b]}, \quad k_5 = \frac{[d]}{[a][c]}$$

therefore,

(9) (a) Bailey, D. M.; Johnson, R. E.; Albertson, N. F. *Org. Synth.* 618–619. (b) Nishiwaki, E.; Tanaka, S.; Lee, H.; Shibuya, M. *Heterocycles* **1988**, *27* (8), 1945–1952. (c) Higher-ordered binding involving cross-complexation of two DNA duplexes may be further assessed by the gel retardation assay.

(10) Grehn, L.; Ragnarsson, U. *J. Org. Chem.* **1981**, *46*, 3492–3497.

Scheme 6

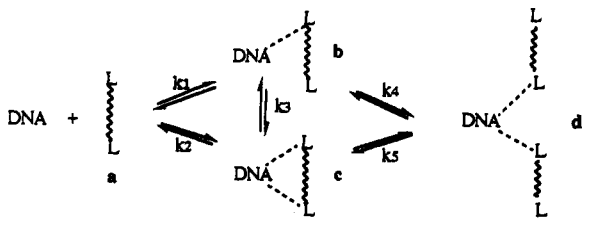

$$k_3 = \frac{[c]}{[b]} = \frac{k_2}{k_1} = \frac{k_4}{k_5} = \alpha$$

The dimensionless quantity α represents the extent of the bidentate binding interaction.

We may define composite binding constants

$$K_{11} = \frac{\{[b] + [c]\}}{[DNA][a]} \quad \text{and} \quad K_{21} = \frac{[d]}{[a]\{[b] + [c]\}}$$

Therefore,

$$K_{11} = k_1 + k_2 = (\alpha + 1)k_1, \quad K_{21} = \frac{1}{1/k_4 + 1/k_5} = \frac{k_4}{(\alpha + 1)}, \quad \text{and} \quad \frac{K_{21}}{K_{11}} = \frac{k_4}{k_1}\frac{1}{(1+\alpha)^2} = \frac{\beta}{(1+\alpha)^2}$$

Here, $\beta = k_4/k_1$, which measures the binding cooperativity of the 2:1 WPPW mode in the absence of the 1:1 bidentate WPPW mode (i.e., $\alpha = 0$).

The equation describing binding isotherms can be written as

$$\gamma = \frac{K_{11}[a] + 2K_{11}K_{21}[a]^2}{1 + K_{11}[a] + K_{11}K_{21}[a]^2} \times \frac{1}{N}$$

γ is the binding density, i.e., the number of ligands bound per base pair and N is the total number of base pairs for the DNA duplex.

Although DNA polymers poly(A)-poly(T) and poly(A-T)-poly(A-T) used in the following CD and ethidium bromide fluorometry studies possess multiple sites, the relationships derived above hold as well, except the binding isotherm equation. Statistical factors influencing the ligand binding to a homogeneous polymeric matrix have been treated by McGhee and von Hippel.[14a] Their equation, shown below, assumes that two neighboring binding sites do not interefere with each other in the process of the binding interaction:

$$\frac{\nu_{ij}}{L_i} = K_{ij}(1 - \sum n_{ij}\nu_i)\left(\frac{1 - \sum n_{ij}\nu_{ij}}{1 - \sum (n_{ij} - 1)\nu_{ij}}\right)^{n_{ij}-1}$$

ν_{ij} is the occupancy for binding mode j of species i, i.e., the average occurrence rate of the binding mode j per base pair, L_i is the free ligand concentration in solution, K_{ij} is the intrinsic binding constant of the binding mode j, and n_{ij} is the binding site size for the particular binding mode j.

In the CD titration studies, the binding isotherm equation can be derived by applying the McGhee–von Hippel equation:

$$\gamma = \frac{k_1[a](ff)^3 + k_2[a](ff)^4 + 2K_{11}K_{21}[a]^2(ff)^4}{1 + 4k_1[a](ff)^3 + 5k_2[a](ff)^4 + 5K_{11}K_{21}[a]^2(ff)^4}$$

$$(ff) = (1 - 4\nu_b - 5\nu_c - 5\nu_d)/(1 - 3\nu_b - 4\nu_c - 4\nu_d)$$

ν_b, ν_c, and ν_d are occupancies of the 1:1 WPW mode, 1:1 bidentate WPPW mode, and 2:1 WPPW mode, respectively. The stoichiometry discussed here is only a relative term: it is the number of ligands to the number of interacting binding sites. Binding site sizes of the WPW mode and WPPW modes are taken as four[7b] and five.[3-5] The complexity of this equation precludes the possibility of curve fitting analysis to obtain binding constants.

In the ethidium bromide fluorescence displacement studies, four equations describing the binding equilibria are as follows: $\nu_{EBr}/([EBr]_t - [DNA]\nu_{EBr}) = K_{EBr}(1 - 2\nu_{EBr} - 4\nu_b - 5\nu_c - 5\nu_d)^2/(1 - \nu_{EBr} - 3\nu_b - 4\nu_c - 4\nu_d)$, $\nu_b/([a]_t - [DNA](\nu_b + \nu_c + 2\nu_d)) = k_1(1 - 2\nu_{EBr} - 4\nu_b - 5\nu_c - 5\nu_d)^4/(1 - \nu_{EBr} - 3\nu_b - 4\nu_c - 4\nu_d)^3$, $\nu_c/([a]_t - [DNA](\nu_b + \nu_c + 2\nu_d)) = k_2(1 - 2\nu_{EBr} - 4\nu_b - 5\nu_c - 5\nu_d)^5/(1 - \nu_{EBr} - 3\nu_b - 4\nu_c - 4\nu_d)^4$, and $\nu_d/([a]_t - [DNA](\nu_b + \nu_c + 2\nu_d))^2 = K_{21}K_{11}(1 - 2\nu_{EBr} - 4\nu_b - 5\nu_c - 5\nu_d)^5/(1 - \nu_{EBr} - 3\nu_b - 4\nu_c - 4\nu_d)^4$ where $[a]_t$ is the total ligand concentration and $[EBr]_t$ is the total ethidium bromide concentration. These four equations describe the binding competition among ethidium bromide, the 1:1 WPW mode, 1:1 bidentate WPPW mode, and the 2:1 WPPW mode. The binding site size of ethidium bromide is taken as two, following the neighboring exclusion rule. Again, the complexity of these relationships prevents the curve fitting analysis from being performed. An alternative way of deriving binding constants is elaborated in the following ethidium bromide fluorometry section.

So far in this model-building analysis, we have not considered the fourth possibility of binding, the cross-complexation of two DNA duplexes by dimeric lexitropsins. This can be justified by analogy with cross-linked bisintercalators. Bisintercalators, with long flexible linkers and binding moieties of binding strengths similar to minor groove binding moieties in our use, usually have both binding moieties bound only to the same duplexes.[11a-e] Bisintercalators with short and rigid linkers capable of completely preventing the interaction of the other binding moiety to the same duplex give only minimal true cross-complexation of two polymeric duplexes.[11f] Probably, the extensive cross-complexation between polymeric DNA duplexes requires a rather strict alignment of DNA duplexes, which is very unfavorable in terms of entropy. As shown in the ethidium bromide displacement analysis, large binding constants of the 1:1 stoichiometry mode for dimeric lexitropsins of pentakis(methylene), hexakis(methylene), and heptakis(methylene) linkages render other high-ordered binding modes completely negligible.[9c]

Circular Dichroism. Circular dichroism is a very useful tool in elucidating interactions between minor groove binders and DNA.[12a] Using CD titration, Zimmer et al.[2] were able to show that distamycin and its analogues interact differently with the alternating polymer poly(dA-dT)-poly(dA-dT) and the homopolymer poly(dA)-poly(dT), inferring that the alternating polymer may accommodate the WPPW binding motif and the homopolymer can only interact in the WPW mode. With $d(ATATAT)_2$ hexamer as the core sequence for NMR titration studies, Wemmer et al.[3c] clearly demonstrated a positive cooperative interaction between the oligonucleotide and two molecules of distamycin in the WPPW mode. For distamycin, and its analogues, the characteristic induced Cotton effect with poly(dA-dT)-poly(dA-dT) appears at around 330 nm, which is distinct from the positive Cotton effect of B-DNA at 260 nm.[2] Therefore, it can be conjectured that CD titration studies with the alternating AT polymer would be informative.

For the series of monomer **8** and compounds **1a–d**, the positive peaks at 260 nm change only to a small extent throughout titration

(11) (a) LePecq, J.-B.; LeBret, M.; Barbet, J.; Roques, B. *Proc. Natl. Acad. Sci. U.S.A.* **1975**, *72*, 2915–2919. (b) Cannellakis, E. S.; Shaw, Y. H.; Hanners, W. E.; Schwartz, R. A. *Biochim. Biophys. Acta* **1976**, *418*, 277–289. (c) Gaugain, B.; Barbet, J.; Oberlin, R.; Ropues, B. P.; LePecq, J.-B. *Biochemistry* **1978**, *17*, 5078–5088. (d) LePecq, J.-B.; Roques, B. P. *Mechanisms of DNA Damage and Repair: Implication for Carcinogenesis and Risk Assessment*; Simic, M. G., Grossman, L., Upton, A. G., Eds.; Plenum Press: New York, 1986; pp 219–244. (e) Welsh, J.; Cantor, C. R. *J. Mol. Biol.* **1987**, *198*, 63–71. (f) Annan, N. K.; Cok, P. R.; Mullins, S. T.; Lowe, G. *Nucleic Acids Res.* **1992**, *20* (5), 983–990.

(12) (a) Zimmer, C.; Luck, G. *Advances in DNA Sequence Specific Agents*; JAI Press Inc.: London, 1992; Vol. 1, p 51–88. (b) Because lexitropsins also have a very intense absorption peak at 240 nm, the interpretation of the CD peak at 260 nm is difficult.

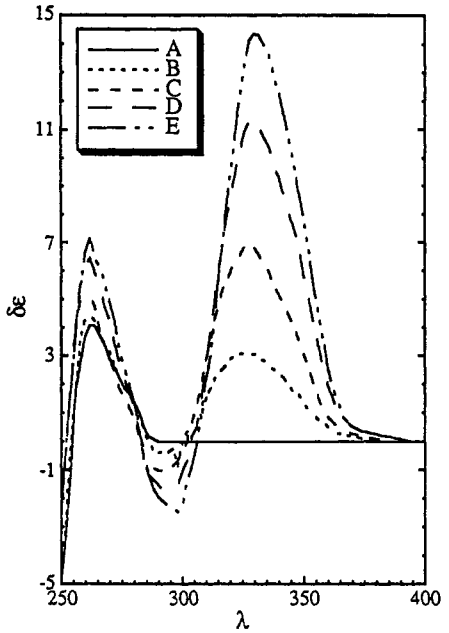

Figure 1. CD titration spectra of monomer **8**. Specific differential extinction coefficient $\delta\epsilon$ (M^{-1} cm^{-1}) is obtained by dividing the measured ellipticity by the poly(A-T)-poly-(A-T) DNA concentration (per nucleotide, ~80 μM) and path length (1.00 cm). γ' is the number of ligands per nucleotide. Spectra A, B, C, and D correspond to γ' values equal to 0, 0.50, 1.10, and 1.70, respectively. Spectrum E corresponds to γ' equal to 2.2.

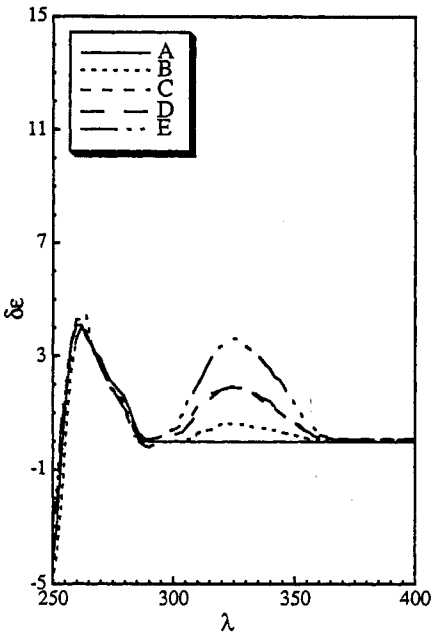

Figure 2. CD titration spectra of dimer **1c**. Specific differential extinction coefficient $\delta\epsilon$ (M^{-1} cm^{-1}) is obtained by dividing the measured ellipticity by the poly(A-T)-poly(A-T) DNA concentration (per nucleotide, ~80 μM) and path length (1.00 cm). γ' is the number of ligands per nucleotide. Spectra A, B, C, and D correspond to γ' values equal to 0, 0.50, 1.10, and 1.70, respectively. Spectrum E corresponds to γ' equal to 2.5.

with no particular characteristic, which is usually the case for minor groove binders.[12b] All of them show positive induced peaks at ~330 nm consistently increase with little drifting of the maximum, characteristic of minor groove binding poly(pyrrolecarboxamide) lexitropsins. CD titration spectra are illustrated in Figures 1 and 2 with monomer **8** and the hexakis(methylene)-linked dimer **1c**. To facilitate comparison among these compounds, the specific extinction coefficient ($\delta\epsilon$) at 330 nm is plotted against γ', the number of added ligands per nucleotide, to construct CD titration curves.[2] $\delta\epsilon = \theta/[\mathrm{DNA}]l$, where θ is the measured

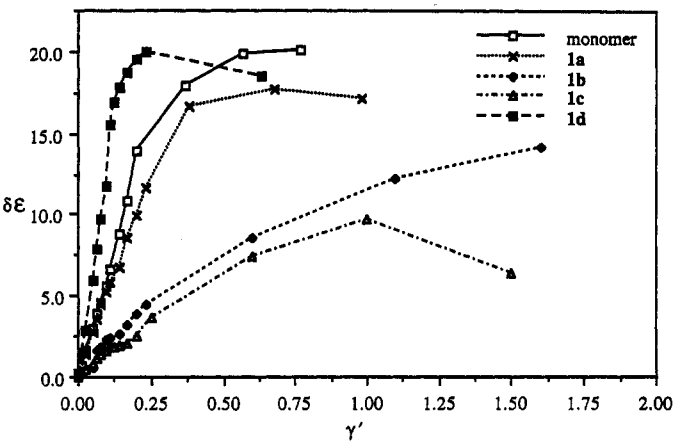

Figure 3. CD titration curves with poly(A-T)-poly(A-T) DNA. The monitoring wavelength is set at 330 nm. For **1c,d**, the precipitation of DNA out of solution at the end of the titration was observed. The decrease of $\delta\epsilon$ is obvious from their titration curves.

ellipticity in degrees, DNA concentration is per nucleotide in M, and the path length l is in cm. For the monomer **8** and the tetrakis(methylene)-linked dimer **1a**, their titration curves in Figure 3 show close similarity in shape and variation (e.g., coincident up to $\gamma' = 0.1$ and with similar end levels), indicating that they have very similar binding interactions with the alternating DNA. There is no true bidentate binding for the tetrakis(methylene)-linked dimer **1a**. Because the 1:1 stoichiometry, the WPW mode in these two cases, predominates in the initial stage of titration, the intrinsic differential extinction coefficient for the WPW motif ΔE^{WPW} can be derived: $\Delta E^{\mathrm{WPW}} = \theta^{\mathrm{WPW}}/[\mathrm{C}]^{\mathrm{WPW}}l \approx \theta^{11}/[\mathrm{C}]^{11}l = \Delta E^{11} \approx \theta/[\mathrm{C}]^{t}l = \theta/\gamma'[\mathrm{DNA}]l = \delta\epsilon/\gamma'$. θ^{WPW} and θ^{11} are ellipticities for the WPW motif and 1:1 stoichiometry, respectively; $[\mathrm{C}]^{\mathrm{WPW}}$, $[\mathrm{C}]^{11}$, and $[\mathrm{C}]^{t}$ are concentrations of the WPW motif and the 1:1 stoichiometry and the total ligand concentration; ΔE^{11} is the composite extinction coefficient for the 1:1 stoichiometry. Therefore, ΔE^{WPW} can be obtained from initial slopes of two titration curves as 60 and 58 $M^{-1}cm^{-1}$, respectively. At the end of the titration, the 2:1 WPPW mode becomes dominant and starts to saturate the DNA matrix. The intrinsic differential extinction coefficient for the WPPW motif ΔE^{WPPW} can be derived: $\Delta E^{\mathrm{WPPW}} = \theta^{\mathrm{WPPW}}/[\mathrm{C}]^{\mathrm{WPPW}}l = \theta^{\infty}/([\mathrm{DNA}]/10)l = 10\delta\epsilon^{\infty}$. θ^{WPPW} and θ^{∞} are the ellipticity for the WPPW motif and the saturation ellipticity, respectively, while $[\mathrm{C}]^{\mathrm{WPPW}}$ and $\delta\epsilon^{\infty}$ are the WPPW motif concentration and the saturation specific differential extinction coefficient. Again, it is assumed that the WPPW motif occupies five base pairs. ΔE^{WPPW} can be estimated to be over 200 and 170 M^{-1} cm^{-1} for monomer **8** and dimer **1a**. The somewhat decreased ΔE^{WPPW} value for dimer **1a** reflects a small appendage effect due to the unbound moiety on the WPPW mode. This decrease, in combination with K_{21} enhancement shown in the following ethidium fluorometry section, results in a smaller contribution to the specific differential extinction coefficient $\delta\epsilon$ from the 2:1 WPPW mode and correspondingly a kink point at $\gamma' = 0.10$, as evidenced from inspection of the CD titration binding isotherm equation. The ΔE^{WPPW} is approximately three times the ΔE^{WPW}, which is not surprising because the effective chromophore concentration is doubled in the 2:1 WPPW motif. This also means that both peptides comprising the antiparallel side by side motif adopt the handedness of the B-DNA without additional distortion. The ΔE^{WPPW} thus derived for the unconnected WPPW motif is an important characteristic of the ideal strainless state: the state of no linkage constraint. An ideal linker should permit two binding moieties to fit comfortably into the groove, resulting in the intrinsic differential extinction coefficient for the covalently connected WPPW motif, ΔE^{WPPW}, and therefore ΔE^{11} very close to this ideal value.

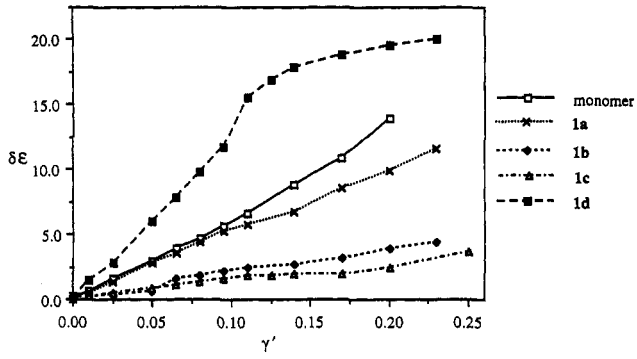

Figure 4. CD titration curves with poly(A-T)-poly(A-T) DNA (close-up).

The titration curves of pentakis(methylene)- and hexakis(methylene)-linked dimers **1b,c** demonstrate significant departure from those of monomer **8** and dimer **1a** (Figures 3 and 4), suggesting that a transition of binding interaction has taken place. This transition also provides another strong supporting evidence of the above assertion that the tetrakis(methylene)-linked dimer **1a** does not have a true bidentate WPPW binding interaction with the alternating AT DNA polymer. The ΔE^{11} values, obtained from the initial slopes of the titration curves, have dropped significantly to 14 and 16 M^{-1} cm^{-1}, respectively. Since $\Delta E^{11} = \Delta E^{WPW}[C]^{WPW}/[C]^{11} + \Delta E^{WPPW}[C]^{WPPW}/[C]^{11}$, two possibilities can be considered: one is that the monodentate WPW binding has a radically different structure leading to a lower ΔE^{WPW} while still the dominant species; the other is that the bidentate binding becomes the dominant species and possesses a much more reduced ΔE^{WPPW} than the ideal value because the shortness of the linkers does not permit snug fitting of both binding moieties. As shown from the ethidium bromide fluorescence displacement experiments, the monodentate WPW binding of the cross-linked molecules does not appear to be much different from that of the monomer **8**; the first proposal is rejected. The titration curves of **1b,c** have flattened regions close to the point after addition of 1 equiv of the ligand ($\gamma' = 0.10$). This is particularly evident for **1c** (Figure 4). This can only be possible when $K_{11}/K_{21} \gg 1$, i.e., $\alpha \gg 1$, from inspection of the CD titration binding isotherm equation. In other words, the binding of 1:1 stoichiometry becomes very difficult to displace. It is evident from the titration curves that the approach to saturation is drastically slowed down. The contribution to 1:1 stoichiometry binding from the bidentate binding mode is therefore significant in these cases. It can be envisaged that a longer linked may then allow a much more comfortable fitting and lead to recovery of ΔE^{11}. This is indeed the case. The heptakis(methylene)-linked dimer **1d** shows a titration curve even above those curves of the monomer **8** and the dimer **1a**, indicating another transition of the binding interaction. The ΔE^{11} value is estimated to be 120 M^{-1} cm^{-1} from the initial slope. This value is dramatically larger than those for the pentakis(methylene)- and hexakis(methylene)-linked dimers **1b,c** and significantly larger than those for monomer **8** and dimer **1a**. However, ΔE^{11} and therefore ΔE^{WPPW} are still falling short of the ideal value of the perfectly fit WPPW motif. Leveling of the titration curve for dimer **1d** appears at $\gamma' = 0.20$ instead of 0.10, which is unexpected from the corresponding neighbor-noninterfering McGhee–von Hippel equation. Quite likely, the great binding strength of dimer **1d** to the alternating AT polymer leads to a rapid saturation of the DNA matrix, thus introducing significant neighboring interactions other than a pure statistical factor. Titration curves of dimers **1c,d** with longer cross-linkers demonstrate obvious decline at the relatively high γ' region, where turbidity started to be observed experimentally. Therefore, the aggregation of DNA polymers and ligands is more significant when excessive free ligands become available in solution. Due to these possible complicating factors in the high-γ' region, information extracted from the low-γ' region (e.g., $\gamma' < 0.05$) is more meaningful for dimers possessing longer linkers. This places a limit on the quantitative use of CD titration curves.

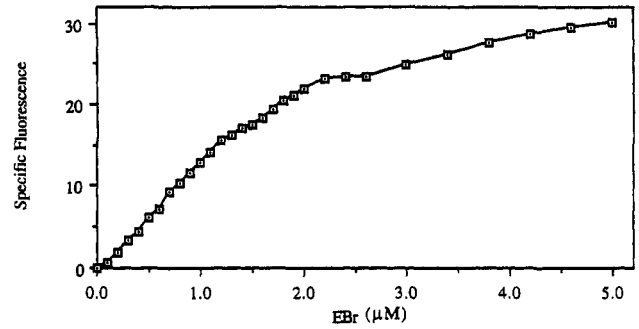

Figure 5. Ethidium bromide self-quenching test for poly(dA)-poly(dT). The relative specific fluorescence is the difference of fluorescence readings in the presence and absence of the DNA (1.00 μM per nucleotide, sensitivity range ×30, sensitivity control ×8).

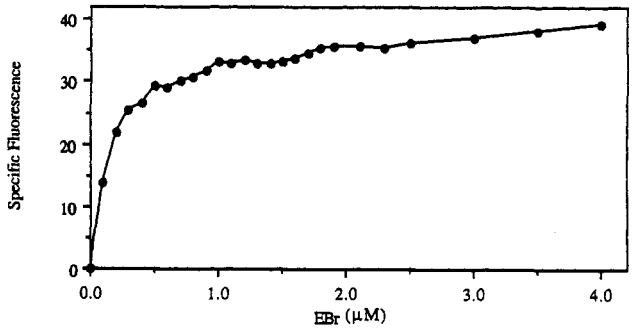

Figure 6. Ethidium bromide self-quenching test for poly(dA-dT)-poly(dA-dT). The relative specific fluorescence is the difference of fluorescence readings in the presence and absence of the DNA (1.00 μM per nucleotide, sensitivity range ×30, sensitivity control ×5).

Ethidium Bromide Fluorometry. Constants for Binding of Ethidium Bromide to Polymeric DNA's and Assessment of Self-Quenching. To further confirm the binding interactions, ethidium bromide fluorescence displacement experiments were carried out. The nonspecific binding to DNA, coupled with the more than a 25-fold enhancement in fluorescence intensity upon binding, makes ethidium bromide a valuable probe of DNA structures and drug binding processes.[13] However, the self-quenching of ethidium bromide due to the nonintercalative second binding mode on the surface of the DNA[13b,c] has to be assessed. The relationship between the difference fluorescence intensity versus total ethidium concentration was determined under our experimental conditions (ionic strength of 0.020 M) for both poly(dA)-poly(dT) and poly(dA-dT)-poly(dA-dT) as shown in Figures 5 and 6. Instead of the sharp decline of fluorescence observed after addition of 1.0 equiv of ethidium bromide (1 molecule per two base pairs) at a lower ionic strength of 0.0010 M,[13b,c] both difference fluorescence titration curves keep growing during the titration although very slowly in the end. Using the nearest neighbor exclusion rule for intercalation and the McGhee–von Hippel equation,[14a,d] which takes into account the statistical factor for binding to DNA polymers, the experimental curves can be very well fitted by applying nonlinear regression analysis, thus proving the negligible extent of self-quenching under the experimental conditions. The McGhee–von Hippel equation describing the binding equilibrium of ethidium bromide is $\nu/([EBr]_t - 0.5\nu) = K_{EBr}(1 - 2\nu)^2/(1 -$

(13) (a) Morgan, A. R.; Lee, J. S.; Pulleyblank; Murry, N. L.; Evans, D. H. *Nucleic Acids Res.* **1979**, *7* (3), 547–69. (b) Waring, M. J. *J. Mol. Biol.* **1965**, *13*, 269–282. (c) LePecq, J. B.; Paoletti, C. *Ibid.* **1967**, *27*, 87–106. (d) Cain, B. F.; Baguley, B. C.; Denny, W. A. *J. Med. Chem.* **1978**, *21* (7), 658.

(14) (a) McGhee, J. D.; von Hippel, P. H. *J. Mol. Biol.* **1974**, *86*, 469–489. For other related analysis, see: (b) Crothers, D. M. *Biopolymers* **1968**, *6*, 575–584. (c) Zasedatelev, A. S.; Gurskii, M. V.; Vol'kenshtein, M. V. *Mol. Biol.* **1971**, *5*, 194–198, 385–393. (d) Shellman, J. A. *Isr. J. Chem.* **1974**, *12* (1–2), 219–238. For an updated review on this subject, see: (e) Lohman, T. M.; Bujalowski, W. *Methods Enzymol.* **1991**, *208*, 258–290.

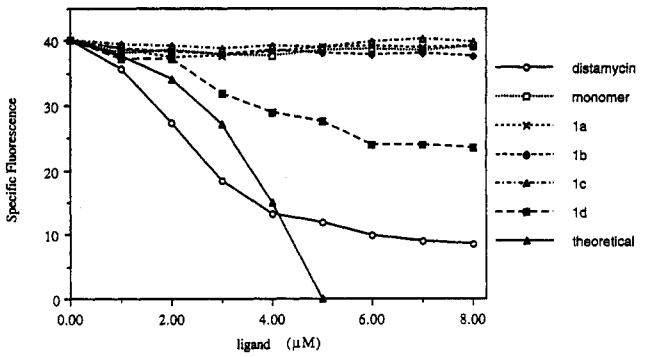

Figure 7. Fluorescence quenching assays for poly(dA)-poly(dT). The relative specific fluorescence is the fluorescence reading with the DNA solution (40.0 μM per nucleotide) as a blank. Ethidium bromide (0.10 μM), sensitivity range (×30), and sensitivity control (×11) were maintained in all experiments.

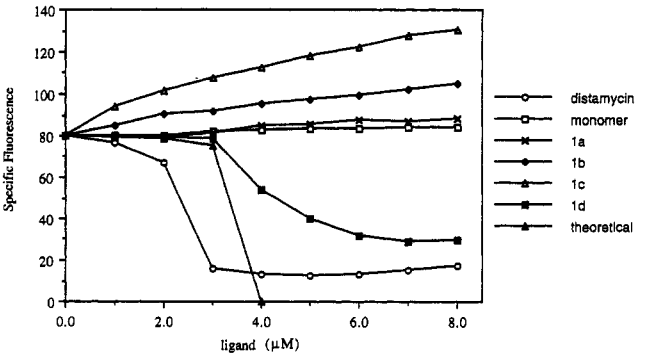

Figure 8. Fluorescence quenching assays for poly(dA-dT)-poly(dA-dT). The relative specific fluorescence is the fluorescence reading with the DNA solution (40.0 μM per nucleotide) as a blank. Ethidium bromide (0.10 μM), sensitivity range (×30), and sensitivity control (×11) were maintained in all experiments.

ν). This equation can be converted into the following equation representing the titration curve: $[EBr]_t = F(f - F)/(K_{EBr}(f - 2F)^2) + 0.5F/f$. Here, $[EBr]_t$ is the total ethidium bromide concentration in μM, K_{EBr} is the binding constant in $10^6 M^{-1}$, F is the specific fluorescence, and f is the constant relating F to the ethidium bromide occupancy ν, i.e., $\nu = F/f$.[13c] Binding constants are derived as 0.23×10^6 M^{-1} (correlation coefficient $R = 0.99$) and 4.3×10^6 M^{-1} (correlation coefficient $R = 0.95$) for poly(dA)-poly(dT) and poly(dA-dT)-poly(dA-dT), respectively. These values are consistent with ones obtained by Baguley et al.[15a] at an ionic strength of 0.010 M and the relationship between ionic strength and binding constants.[15b]

Ethidium Bromide Fluorescence Quenching Assay. The fluorescence quenching effect of added binders also needs to be evaluated. The fluorescence quenching assay by Baguley et al.[15c] was used to screen distamycin, monomer **8**, and dimers **1a–d** with poly(dA)-poly(dT) and poly(dA-dT)-poly(dA-dT) DNA's (Figures 7 and 8). Theoretical curves for a nonquenching binder with infinite binding strength are calculated, which serve as reference for diagnosing the extent of quenching. For poly(dA)-poly(dT), all compounds except distamycin had titration curves well above the corresponding theoretical curves, indicating little quenching. For poly(dA-dT)-poly(dA-dT), an interesting quenching pattern was observed. Monomer **8** and the tetra-/heptakis-(methylene)-linked dimers did not show any quenching, while the penta-/hexakis(methylene)-linked dimers consistently enhanced fluorescence. This characteristic plausibly has a common structural origin as the unique CD ΔE[11] decrease of these two compounds. Again, distamycin demonstrated strong fluorescence quenching, which is in contrast to minor groove binding bisquaternary ammonium heterocycles.[15d] The heptakis(methylene)-linked dimer **1d** appeared to displace ethidium bromide in the later part of both titrations, indicating it is a stronger binder than other dimers in this series.

Ethidium Bromide Fluorescence Displacement Experiment. Displacement experiments were carried out to determine the required total ligand concentration to achieve a 50% reduction in fluorescence intensity, the so-called C_{50}. An apparent binding constant defined as $K_{app} = K_{EBr}C_{EBr}/C_{ligand}$ can be calculated, following the literature convention.[13a] As will be shown below, this quantity greatly underestimates the intrinsic binding strength in a highly heterogeneous manner, even without fluorescence quenching by ligands and, as a result, comparison with ethidium bromide is impossible and very likely misleading.

Our proposed data treatment is based on the four McGhee–von Hippel equations discussed in the Construction of the Binding Model. The initial binding status of ethidium bromide to the DNA polymer before addition of the binder is first calculated. At 50% ethidium bromide displacemnent, the bound ethidium bromide is one-half of the initial bound concentration and the free ethidium bromide concentration in solution can be obtained accordingly. Using the equation for ethidium bromide, the occupancy of a putative single-mode binder with a binding site size of five base pairs for poly(dA-dT)-poly(dA-dT) and four base pairs for poly(dA)-poly(dT)[7b] is determined. The occupancy derived is placed into the corresponding equation describing the binder, and a relationship between the intrinsic binding constant K and C_{50} value (in μM) can be derived as a hyperbolic function: $K = (91.1 \times 10^6)/(C_{50} - 0.0487)$ M^{-1} and $K = (0.857 \times 10^6)/(C_{50} - 0.0554)$ M^{-1} for poly(dA-dT)-poly(dA-dT) and poly(dA)-poly(dT), respectively.[15e] As can be conjectured, K_{app} is much smaller than the intrinsic binding constants by 21 and 4 times for poly(dA-dT)-poly(dA-dT) and poly(dA)-poly(dT), respectively, when C_{50} is much larger than 0.0487 and 0.0554 μM. This is because under the experimental conditions the DNA matrix is highly occupied by ligand and therefore the statistical effect is very pronounced. When the C_{50} value is close to 0.0487 and 0.0554 μM, the K_{app} deviates even more and can be up to thousands of times below the intrinsic binding constant. Such a result is in stark contrast to what is expected from the K_{app} calculation which would give a saturated value under this circumstance.[13a,d] Heterogeneity of this nature makes it misleading to qualitatively compare the binding strength of the same series by using the K_{app} formalism. We stress this problem because, in our opinion, an increasing number of publications concerning minor groove binders employ this simple formalism without due caution. To determine binding constants more accurately for strong binders, we recommend that an ethidium bromide concentration higher

(15) (a) Baguley, B. C.; Falkenhaug, E.-M. *Nucleic Acids Res.* **1978**, *5* (1), 161–171. (b) Wilson, W. R.; Baguley, B. C.; Wakelin, L. P. G.; Waring, M. J. *Mol. Pharmacol.* **1981**, *20*, 404–414. (c) Baguley, B. C.; Denny, W. A.; Atwell, G. J.; Cain, B. F. *J. Med. Chem.* **1981**, *24*, 170–177. (d) Denny, W. A.; Atwell, G. J.; Baguley, B. C.; Cain, B. F. *J. Med. Chem.* **1979**, *22* (2), 134. (e) A single-mode binding requires only one data point from the ethidium fluorescence titration curve to derive the binding constant if the quenching effect is properly corrected. If one mode becomes dominant in a complicated binding interaction, the corresponding binding constant can be readily estimated using the C_{50} value. Reassessment can be then carried out to determine the degree of domination and therefore the accuracy of such an estimation. Starting with a good initial estimation, we may conduct a grid search for optimal set of binding constants which fit well into a few selected data points, e.g., 25%, 35%, and 50% ethidium displacement points. The minimal number of data points required is equal to the number of binding modes. K_{21}'s for **1b–d** are so small compared with K_{11} that no attempts were made to further improve the initial estimation by adding yet another data point. Under the experimental conditions, ethidium bromide and DNA have total concentrations of 1.26 μM and 1.00 μM per nucleotide, respectively. $[a]_t$ is the total concentration of the ligand in μM; binding constants k_1, k_2, K_{11}, and K_{21} are in 10^6 M^{-1}. (f) The self-quenching is less of a problem compared with binder quenching because the ethidium displaced from the DNA matrix is approximately 0.1 μM, which is much less than the existing free ethidium in solution ($\sim$1.24 μM) and therefore has very little effect on self-quenching. It seems worthy to measure the second binding mode of ethidium to DNA quantitatively. (g) Proton NMR signals of these dimeric molecules are broadened in the aqueous solution, suggesting the occurrence of stacking.

Table 1. Constants of Binding to poly(dA)-poly(dT)

compd	8	1a	1b	1c	1d
C_{50} (μM)	0.45	0.89	1.38	0.35	0.13
K ($\times 10^6$)	2.17	1.03	0.65	2.91	11.5

Table 2. Constants of Binding to poly(dA-dT)-poly(dA-dT)

compd	8	1a	1b	1c	1d
C_{50} (μM)	2.08	1.41	2.05	0.87	0.098
C_{25} (μM)	1.05	0.69	0.93	0.26	0.048
K_{11} ($\times 10^6$)	2.00	3.19	48.7	113	1842
K_{21} ($\times 10^6$)	10.4	16.6	1.09	0.46	0.029

than the usual 1.26 μM be used. In addition, both ethidium bromide self-quenching and binder quenching effects should be evaluated.[15f]

It has been determined that the poly(dA)-poly(dT) homopolymer interacts with minor groove binders only in the WPW mode,[2] probably due to its inherently narrower minor groove.[3c] Binding constants calculated from C_{50} values are therefore straightforward and are shown in Table 1. Overall, binding constants change to a relatively small extent. The binding constants of **1a,b** decrease somewhat compared with that of monomer **8**, probably reflecting the necessity of unpacking stacked dimeric structures of ligands in the aqueous solution.[15g] The binding constants of **1c,d** become larger than that of monomer **8**, plausibly because longer linkers permit favorable electrostatic interactions between the positively charged outer ligand moieties and negatively charged sugar phosphate backbones of DNA, compensating for the unpacking free energy cost. Overall, these dimeric lexitropsins do not interact with DNA significantly different from the corresponding monomer in the WPW mode. In other words, the large outer appendage appears to have no significant effect on the WPW mode binding interaction.

C_{50} values and intrinsic binding constants of monomer **8** and **1a–d** with poly(dA-dT)-poly(dA-dT) are listed in Table 2. For weaker binders monomer **8** and dimer **1a**, which do not have the 1:1 WPPW mode, the WPPW binding mode of 2:1 stoichiometry dominates under the experimental conditions. A formula relating k_1 and k_4 to C_{50} can be derived from McGhee–von Hippel equations as $k_1k_4 \approx 91.1 \times 10^{12}/(C_{50} - 0.0487)$.[2] k_1 and k_4 correspond to K_{11} and K_{21}, respectively, due to absence of the 1:1 WPPW bidentate binding mode. This formula can be used for estimating k_1 and k_4 of monomer **8** and dimer **1a** initially. For example, the k_1 of monomer **8** is initially assumed to be the same for poly(dA)-poly(dT) and poly(dA-dT)-poly(dA-dT) to give the first estimation of k_4.[16] A refinement calculation is then conducted to fit the C_{25} value.[15e] k_1 and k_4 of **1a** are somewhat larger than those of monomer **8**. For dimeric binders **1b–d**, which have dominant 1:1 WPPW bidentate binding, K_{11} is estimated from C_{50} to a first approximation and the corresponding α value is derived from $\alpha = (K_{11}/k_1) - 1$, assuming k_1 remains unchanged for **1a–d**. The composite constant K_{21} ($=k_4/(1 + \alpha)$) is then calculated assuming k_4 remains unchanged for **1a–d**. All these estimations could be then refined by reiterative calculation to fit two data points, C_{50} and C_{25}.[15e] Due to large α values for all three compounds, further refinement seems unnecessary and was not attempted. Correction of the ligand quenching effect[15c] appears unnecessary from the above quenching studies. As is shown, the binding strength of the 1:1 mode increases rapidly from **1a** to **1d** while that of the 2:1 mode decreases at the same time. The binding strength of **1d** is 920 times larger than that of the monomer **8** in the 1:1 mode.

Discussion

The above binding studies indicate that 1:1 bidentate binding with the WPPW motif plays an important part in contributing to the overall stability of the 1:1 stoichiometry. The ratio of bidentate to monodentate binding (i.e., α) can be estimated to be 15, 35, and 577 for **1b**, **1c**, and **1d**, respectively. The binding of the 2:1 stoichiometry is normally greatly disfavored. However, the ΔE^{11} value is not fully recovered even for the best fit case **1d** and the binding constant has not yet reached the maximal value. Search for the ideal cross-linker is a worthwhile objective. Despite these concerns, the concept of central cross-linkage design is basically sound. Further characterization and analysis by NMR spectroscopy, molecular modeling, footprinting, gel retardation assay, and cytotoxicity assay against tumor cells are currently underway in our group.

It is interesting to compare the correspondence among three different data sets including CD, fluorescence quenching, and binding strength. Both CD and fluorescence quenching reflect **1a** to **1b**, **1b** to **1c**, and **1c** to **1d** transitions in the binding interaction with alternating A-T DNA sensitively, as previously discussed. Can the binding strength also reflect these transitions? We may calculate binding constant ratios between two neighboring cross-linked lexitropsins in this series. K_{11} ratios between **1b** and **1a**, **1c** and **1b**, and **1d** and **1c** are 15, 2.3, and 16, respectively. K_{21} ratios between **1a** and **1b**, **1b** and **1c**, and **1c** and **1d** are 15, 2.3, and 16, respectively. This trend seems to indicate an abrupt transition between **1b** and **1a**, a smooth transition between **1c** and **1b**, and an abrupt between **1d** and **1c** again. Therefore, a fairly good correspondence among all three sets of data appears to exist. This correspondence supports the rigor of our binding analysis.

It can be observed that a reasonably good fit is not available until the linkage reaches the length of six consecutive carbon–carbon single bonds. The corresponding maximal contour length is 7.53 Å, which is much longer than the distance between nitrogen atoms of two π–π stacked pyrrole rings. Probably, staggering and different orientations of two central pyrrole planes in the two tris(pyrrolecarboxamide) binding moieties can increase the distance between two nitrogen atoms substantially. Quite likely, orientations of two C–N single bonds in the termini of the poly(methylene) chain impose another constraint which was not taken into account initially. Another factor not considered in the initial design is the self-coiling of the poly(methylene) chain in water due to hydrophobicity, which will also reduces the end to end distance of the chain. Perhaps, these poly(methylene)-linked lexitropsins are actually preorganized in a certain way in water when both stacking of two binding units and the self-coiling of poly(methylene) chains are all functioning.

In this article, we introduce some refinements into the CD and ethidium fluorometry data analyses. We believe that the "strainless" ΔE^{WPPW} value is meaningful in diagnosing the degree of fitting between dimeric lexitropsin and DNA. Deviation from this value, either lower or higher, reflects the linkage effect: change of the ligand–DNA complex geometry from the strainless ideal geometry. Comparison of the experimentally derived ΔE^{11} with this value will serve to guide the linkage optimization process. Strainless induced differential extinction coefficients of this type may find application in analyzing the conjugate binder–DNA interaction, for example, the end to end linked lexitropsin–DNA interaction. The alternative way of ethidium bromide fluorescence displacement data treatment provides the more meaningful intrinsic binding constant instead of the conventional apparent binding constant. Experimentally, the ethidium bromide fluorometry remains simple since only quenching assay experiments need to be implemented in addition to the normal procedure. Overall, this highly sensitive method allows a rapid assessment of binding interactions between DNA polymers and cross-linked lexitropsins.

As more information becomes available, the next generation of cross-linked lexitropsins, including asymmetric ones, can be designed and engineered with greater precision. Longer poly(methylene) linkers still have to be explored further to realize the

(16) Zimmer, C.; Wahnert, U. *Prog. Biophys. Mol. Biol.* **1986**, *47*, 31–112.

full potential of this kind of simple linkage. Rigidity, hydrophilicity, and chirality of linkers are important considerations in search of ideal cross-linkers. While there is no reason why a single central cross-linkage cannot serve in connecting two much longer lexitropsin binding moieties as well as in connecting shorter ones, longer lexitropsins containing several cross-linkages will generate ladderlike structures which may have high specificity for longer base sequences due to greater preorganization. The observed much higher binding strength of cross-linked lexitropsins in comparison with the monomer may also provide room for structural maneuvering aiming at improvement of sequence specificity. Predominance of the WPPW bidentate binding interaction and possible modulation of the interaction through systematic change of the cross-linkage may render some cross-linked lexitropsins useful for probing DNA structures. It must be noted that functionalization of these "carriers" may present a unique opportunity of making close mimics of restriction enzymes since hydrolytic functional groups may be attached symmetrically along two binding fragments and simultaneous strand specific double-strand cleavage may produce similar cleavage patterns as natural enzymes. These hydrolytic functional groups can be just some nonspecific natural enzymes. Because not all palindromic sequences are recognized by restriction endonucleases,[17] expansion of recognizable sequences by synthetic enzyme mimics may be even envisaged.[18] With multiple oxidative functional groups attached, high cytotoxic potency may be expected because of greatly improved binding strength and multiple simultaneous double-strand damages, i.e., segmental removal of short DNA duplexes.

Experimental Section

A buffer solution (pH = 7.00) containing Tris-HCl (10.0 mM) and sodium chloride (10.0 mM) was prepared with distilled deionized water. This buffer was used in the preparation of all DNA and ligand stock solutions. DNA polymers were purchased from the Sigma Co. and stored at −20 °C.

Circular dichroism was measured on Jasco-ORD/UV5 at 23 °C. The concentration of DNA was determined from UV absorption at 260 nm with ϵ_{260} = 6750 and 6000 for poly(dA-dT)-poly(dA-dT) and poly(dA)-poly(dT), respectively. The DNA concentration per nucleotide was maintained at ~80 μM for all titrations while the concentration of ligand was 20 times this value. Fluorescence was measured on a Turner spectrofluorometer model 430. Circulating water at 23 °C was passed through the measurement chamber during experimentation. Excitation and emission wavelengths were set at 550 and 600 nm, respectively. Readings were taken five times for each ligand concentration to give an average value. For self-quenching and ligand quenching assays, DNA solutions were used as a blank. The DNA concentration per nucleotide was 1.00 μM in self-quenching assays, while the DNA concentration per nucleotide and the ligand concentrations were maintained at 40.0 and 0.10 μM, respectively, in ligand quenching assays. For displacement experiments, the ethidium bromide solution before addition of DNA was taken as the blank and concentrations of DNA and ethidium bromide were 1.00 μM per nucleotide and 1.26 μM, respectively.

Melting points were determined on a Fisher-Johns apparatus and were uncorrected. UV spectra were taken on a Hewlet-Packard diode array HP8542 spectrophotometer. IR spectra were recorded on a Nicolet magna 750 spectrometer with a Nic-plane microscope. In the IR data presentation, bracketed w, m, s, and vs indicate the extent of absorption as weak, medium, strong, and very strong. ^{1}H-NMR spectra were measured on a Varian 300 instrument with TMS as the internal standard on the ppm scale. Multiplicities of resonance peaks are indicated as singlet (s), doublet (d), triplet (t), broad singlet (bs), quartet (q), and multiplet (m). Electron impact (EI) mass measurement was performed on a Kraytos MS 50 high-resolution mass spectrometer, while fast atom bombardment mass measurement was carried out with AEI MS-9 and MS-50 mass spectrometers using 1,4-dithiothreol (Cleland's reagent) as the matrix. Elemental analysis was performed by the departmental service at the University of Alberta on a Carlo Erba Instruments EA 1108 elemental analyzer.

Nonlinear regression analysis was conducted by using the Inplot 4.01 software of GraphPad Software Inc. on an IBM 486 computer. The grid search analysis of ethidium bromide fluorescence displacement experiments and the theoretical quenching curve calculation were performed with the KaleidaGraph 2.1 software of Abelbeck Software Inc. on a Macintosh IIfx computer, using the series creation function.

In the following section, typical synthetic procedures are illustrated with the hexa(methylene) linkage series.

1,1′-(1,6-Alkanediyl)bis(pyrroles) 2a–d. To a solution of freshly distilled pyrrole (17.4 mL, 0.248 mol) in anhydrous THF were introduced pieces of potassium metal (11.00 g, 0.281 mol) under a nitrogen atmosphere. The solution was refluxed for 5 h, during which time the potassium disappeared and a white suspension resulted. 1,6-Dibromohexane (19.60 mL, 0.126 mol) was added dropwise over 30 min, and the mixture was heated to reflux overnight. The reaction mixture was cooled to room temperature and filtered. The white solid residue was dissolved in water and the solution extracted with ether. The combined organic fractions were concentrated *in vacuo* to give a yellowish oil. Fractional vacuum distillation (0.10 mmHg) furnished **2c** as a colorless oil (22.50 g, 83% yield) at 124–126 °C.

2a: yield 81%; bp 93–95 °C (0.1 mmHg); IR (film) ν_{max} 3094 (w), 2939 (s), 1500 (s), 1281 (s), 732 (s) cm^{-1}; ^{1}H-NMR ($CDCl_3$) δ 1.75 (4H, m), 3.88 (4H, m), 6.15 (4H, t, J = 2.5 Hz), 6.15 (4H, t, J = 2.5 Hz), and 6.64 (4H, t, J = 2.5 Hz); EIMS m/e (relative intensity) 188.1310 (100, M, 188.1314 calcd for $C_{12}H_{16}N_2$), 149 (10), 120 (42), 95 (28), 53 (19).

2b: yield 78%; bp 115–118 °C (0.1 mmHg); IR (film) ν_{max} 3122 (w), 2932 (s), 1500 (s), 1281 (s), 725 (vs) cm^{-1}; ^{1}H-NMR ($CDCl_3$) δ 1.29 (2H, m), 1.78 (4H, m), 3.87 (4H, t, J = 7.2 Hz), 6.15 (4H, t, J = 2.0 Hz), 6.64 (4H, t, J = 2.0 Hz); EIMS m/e (relative intensity) 202.1471 (82, M, 202.1470 calcd for $C_{13}H_{18}N_2$), 134 (10), 122 (24), 81 (100), 53 (19). Anal. Calcd for $C_{13}H_{18}N_2$: C, 77.41; H, 8.91; N, 13.86. Found: C, 77.41; H, 9.26; N, 13.77.

2c: IR (film) ν_{max} 3099 (w), 2930 (s), 2857 (m), 1545 (m), 1500 (m) cm^{-1}; ^{1}H-NMR ($CDCl_3$) δ 1.30 (4H, m), 1.75 (4H, m), 3.84 (4H, t, J = 7.1 Hz), 6.14 (4H, m), 6.63 (4H, m); EIMS m/e (relative intensity) 216.1627 (64, M, 261.1626 calcd for $C_{14}H_{20}N_2$), 123 (33), 81 (100), 53 (19). Anal. Calcd for $C_{14}H_{20}N_2$: C, 77.73; H, 9.32; N, 12.95. Found: C, 77.72; H, 9.28; N, 12.78.

2d: yield 89%; bp 138–140 °C (0.1 mmHg); IR (film) ν_{max} 3100 (w), 2931 (s), 2857 (m), 1500 (m), 722 (vs) cm^{-1}; ^{1}H-NMR ($CDCl_3$) δ 1.32 (6H, m), 1.76 (4H, m), 3.87 (4H, t, J = 6.6 Hz), 6.27 (4H, t, J = 2.4 Hz), 6.87 (4H, t, J = 2.4 Hz); EIMS m/e (relative intensity) 230.1782 (100, M, 230.1783 calcd for $C_{15}H_{22}N_2$), 150 (18), 136 (43), 84 (33), 68 (20).

1,1′-(1,6-Alkanediyl)-2,2′-bis(trichloroacetyl)bis(pyrroles) 3a–d. To the solution of **2c** (5.00 g, 23.1 mmol) in anhydrous dichloromethane (25 mL) was added trichloroacetyl chloride (5.74 mL, 50.8 mmol) over 1 h under nitrogen at room temperature. Rapid evolution of gas was observed. The resulting brown solution was stirred for 24 h. The reaction mixture was filtered rapidly through a small layer of silica gel and dried ($MgSO_4$). Evaporation of the yellowish filtrate *in vacuo* provided **3c** as a light yellow solid (10.30 g, 86% yield).

3a: yield 84%; IR (film) ν_{max} 3107 (w), 2946 (w), 1663 (vs), 1091 (m), 727 (vs) cm^{-1}; ^{1}H-NMR ($CDCl_3$) δ 1.82 (4H, m), 4.35 (4H, t, J = 6.5 Hz), 6.24 (2H, dd, J = 2.0 and 4.2 Hz), 7.03 (2H, t, J = 2.0 Hz), 7.55 (2H, dd, J = 2.0 and 4.2 Hz); EIMS m/e (relative intensity) 479.9108 (1, M, 479.9128 calcd for $C_{16}H_{14}N_2O_2{}^{35}Cl_4{}^{37}Cl_2$), 477.9112 (1, M, 477.9112 calcd for $C_{16}H_{14}N_2O_2{}^{35}Cl_5{}^{37}Cl$), 475.9175 (0.6, M, 475.9186 calcd for $C_{16}H_{14}N_2O_2{}^{35}Cl_6$), 215 (27), 148 (37), 120 (100), 80 (79).

3b: 90%; IR (powder) ν_{max} 3110 (w), 2932 (m), 1667 (vs), 1469 (s), 739 (vs) cm^{-1}; ^{1}H-NMR ($CDCl_3$) δ 1.38 (2H, m), 1.80 (4H, m), 4.32 (4H, t, J = 7.2 Hz), 6.25 (2H, dd, J = 2.0 and 4.5 Hz), 7.02 (2H, dd, J = 1.5 and 2.0 Hz), 7.55 (2H, dd, J = 1.5 and 4.5 Hz); EIMS m/e (relative intensity) 493.9330 (0.33, M, 493.9284 calcd for $C_{17}H_{16}N_2O_2{}^{35}Cl_4{}^{37}Cl_2$), 491.9320 (0.5, M, 491.9313 calcd for $C_{17}H_{16}N_2O_2{}^{35}Cl_5{}^{37}Cl$), 489.9373 (0.2, M, 489.9343 calcd for $C_{17}H_{16}N_2O_2{}^{35}Cl_6$), 346 (22), 134 (100), 81 (88).

3c: mp 139–141 °C; IR (powder) ν_{max} 3117 (w), 2935 (s), 1663 (vs), 1363 (m), 1096 (m) cm^{-1}; ^{1}H-NMR ($CDCl_3$) δ 1.37 (4H, m), 1.77 (4H, m), 4.30 (4H, t, J = 7.3 Hz), 6.22 (2H, dd, J = 2.8 and 4.8 Hz), 7.00

(17) (a) Watson, J. D.; Tooze, J.; Kurtz, D. T. *Recombinant DNA: A Short Course*; Scientific America Books: New York, 1983; pp 248–253. For a compilation of restriction enzymes, see: (b) Roberts, R. J.; Macelis, D. *Nucleic Acids Res.* **1991**, *19s*, 2077–2109.

(18) Demidov, V.; Frank-Kamenetskii, M. D.; Egholm, M.; Buchart, O.; Nielsen, P. E. *Nucleic Acids Res.* **1993**, *21* (9), 2103–2107 and references cited in the article.

(2H, t, J = 2.8 Hz), 7.54 (2H, dd, J = 2.8 and 4.8 Hz); EIMS m/e (relative intensity) 507.9439 (2, M, 507.9440 calcd for $C_{18}H_{18}N_2O_2^{35}Cl_4^{37}Cl_2$), 505.9476 (3, M, 505.9470 calcd for $C_{18}H_{18}N_2O_2^{35}Cl_5^{37}Cl$), 503.9494 (1, M, 503.9499 calcd for $C_{18}H_{18}N_2O_2^{35}Cl_6$), 387 (27), 83 (100).

3d: yield 80%; IR (film) ν_{max} 3150 (w), 2930 (s), 1667 (vs), 1089 (m), 741 (vs) cm^{-1}; ^{1}H-NMR ($CDCl_3$) δ 1.35 (6H, m), 1.74 (4H, m), 4.29 (4H, t, J = 7.2 Hz), 6.23 (2H, dd, J = 2.4 and 4.7 Hz), 7.00 (2H, t, J = 2.4 Hz), 7.52 (2H, dd, J = 2.4 and 4.7 Hz); EIMS m/e (relative intensity) 521.9596 (17, M, 521.9597 calcd for $C_{19}H_{20}N_2O_2^{35}Cl_4^{37}Cl_2$), 519.9627 (21, M, 519.9626 calcd for $C_{19}H_{19}N_2O_2^{35}Cl_5^{37}Cl$), 517.9655 (11, M, 517.9656 $C_{19}H_{20}N_2O_2^{35}Cl_6$), 401 (9100), 142 (87).

1,1′-(1,*n*-Alkanediyl)-2,2′-bis(trichloroacetyl)-4,4′-dinitrobis(pyrroles) 4a–d. A suspension of **3c** (5.00 g) in acetic anhydride–dichloromethane (40 mL, 1:1, v/v) was cooled to −78 °C. To this mixture was introduced fuming nitric acid (1.60 mL, >90%) dropwise for 15 min. The brown mixture was warmed up to room temperature gradually over 35 min and stirred for 3 h. The final reaction mixture was diluted with dichloromethane, neutralized with saturated sodium bircarbonate solution, and dried ($MgSO_4$). A brown foam was obtained after evaporation of solvents *in vacuo*. Silica gel chromatography with petrolium ether and dichloromethane (1:1, v/v) provided **4c** as a yellowish solid (2.85 g, 48% yield).

4a: yield 55%; mp 276–278 °C (dec.); IR (powder) ν_{max} 3141 (w), 2954 (w), 1689 (s), 1317 (vs), 1105 (s) cm^{-1}; ^{1}H-NMR ($CDCl_3$) δ 1.88 (4H, bs), 4.40 (4H, bs), 7.81 (2H, d, J = 1.5 and 2.0 Hz), 8.02 (2H, d, J = 1.5 and 2.0 Hz); EIMS m/e (relative intensity) 569.8824 (0.6, M, 569.8829 calcd for $C_{16}H_{12}N_4O_6^{35}Cl_4^{37}Cl_2$), 567.8866 (0.8, M, 567.8859 calcd for $C_{16}H_{12}N_4O_6^{35}Cl_5^{37}Cl$), 565.8894 (0.3, M, 565.8888 calcd for $C_{16}H_{12}N_4O_6^{35}Cl_6$), 451 (49), 258 (65), 55 (100). Anal. Calcd for $C_{16}H_{12}N_4O_6Cl_6$: C, 33.74; H, 2.11; N, 9.84. Found: C, 33.49; H, 1.98; N, 9.48.

4b: yield 50%; mp 72–74 °C; IR (powder) ν_{max} 3127 (m), 2930 (m), 1681 (s), 1316 (vs), 736 (s) cm^{-1}; ^{1}H-NMR ($CDCl_3$) δ 1.57 (2H, m), 1.93 (4H, m), 4.41 (4H, t, J = 7.8 Hz), 7.85 (2H, d, J = 1.8 Hz), 8.03 (2H, d, J = 1.18 Hz); EIMS m/e (relative intensity) 583.8995 (2.6, M, 583.8986 calcd for $C_{17}H_{114}N_4O_6^{35}Cl_4^{37}Cl_2$), 581.9051 (3.2, M, 581.9015 calcd for $C_{17}H_{14}N_4O_6^{35}Cl_5^{37}Cl$), 579.9037 (2, M, 579.9045 calcd for $C_{17}H_{14}N_4O_6^{35}Cl_4^{37}Cl_2$), 463 (64), 162 (62), 69 (100).

4c: mp 147 °C; IR (powder) ν_{max} 3124 (m), 2943 (m), 1686 (s), 1314 (s), 1105 (m) cm^{-1}; ^{1}H-NMR ($CDCl_3$) δ 1.48 (4H, m), 1.84 (4H, m), 4.38 (4H, t, J = 8.0 Hz), 7.98 (2H, d, J = 1.9 Hz), 7.78 (2H, d, J = 1.9 Hz); EIMS m/e (relative intensity) 597.9134 (6, M, 597.9142 calcd for $C_{18}H_{16}N_4O_6^{35}Cl_4^{37}Cl_2$), 595.9171 (8, M, 595.9172 calcd for $C_{18}H_{16}N_4O_6^{35}Cl_5^{37}Cl$), 593.9215 (4, M, 593.9201 calcd for $C_{18}H_{16}N_4O_6^{35}Cl_6$), 477 (77), 180 (100). Anal. Calcd for $C_{18}H_{16}N_4O_6Cl_6$: C, 36.21; H, 2.70; N, 9.38. Found: C, 36.16; H, 2.49; N, 9.20.

4d: yield 40%; mp 142–143 °C; IR (powder) ν_{max} 3129 (m), 2944 (s), 1694 (vs), 1314 (vs), 743 (vs) cm^{-1}; ^{1}H-NMR ($CDCl_3$) δ 1.39 (6H, m), 1.79 (4H, m), 4.35 (4H, t, J = 7.8 Hz), 7.76 (2H, d, J = 1.9 Hz), 7.97 (2H, d, J = 1.9 Hz); EIMS m/e 611.9267 (0.9, M, 611.9299 calcd for $C_{19}H_{18}N_4O_6^{35}Cl_4^{37}Cl_2$), 609.9314 (1, M, 609.9328 calcd for $C_{18}H_{16}N_4O_6^{35}Cl_5^{37}Cl$), 607.9349 (0.6, M, 607.9357 calcd for $C_{18}H_{16}N_4O_6^{35}Cl_6$), 344 (57), 55 (100).

Tetrapyrrolediamines 5a–d. Platinum oxide (55 mg) was added to *N*-[(dimethylamino)propyl] 1-methyl-4-nitropyrrolecarboxamide (535 mg, 2.11 mmol) in anhydrous methanol (10.0 mL). This mixture was evacuated by the freeze and thaw procedure and then charged with 1 atm of hydrogen. A vigorous stirring was maintained at room temperature for 3 h. The methanol was removed *in vacuo*, and DMF was introduced (5 mL). The DMF solution was concentrated to dryness by using an oil pump and anhydrous DMF reintroduced (5.0 mL). To this DMF solution was then added compound **4c** (597 mg, 1.00 mmol), and stirring was continued for 5 h at room temperature under nitrogen. The crude mixture was chromatographed over a silica gel column with a concentrated ammonia and methanol mixture (1/19, v/v) as the eluent. The desired product **5c** (445 mg, 55%) was obtained as a yellow solid after evaporation of solvents.

5a: yield 56%; IR (powder) ν_{max} 3600–2400 (s, broad), 2943 (s), 1653 (vs), 1437 (s), 1312 (s) cm^{-1}; ^{1}H-NMR (DMSO-d_6) δ 1.60 (4H, m), 1.73 (4H, bs), 2.16 (12H, s), 2.25 (4H, t, J = 7.2 Hz), 3.19 (4H, m), 3.81 (6H, s), 4.45 (4H, bs), 6.79 (2H, J = 1.6 Hz), 7.20 (2H, d, J = 1.6 Hz), 7.60 (2H, d, J = 1.6 Hz), 8.11 (2H, t, J = 5.5 Hz), 8.26 (2H, d, J = 1.6 Hz), 10.75 (2H, s); FABMS m/e (relative intensity) 779 (0.1, M + H), 617 (0.3), 576 (0.9), 544 (0.7), 119 (100); HRFABMS m/e 779.3986 (M + H, 779.3852 calcd for $C_{36}H_{51}N_{12}O_8$).

5b: yield 54%; IR (powder) ν_{max} 3126 (m), 2939 (s), 1640 (s), 1312 (vs), 812 (s) cm^{-1}; ^{1}H-NMR (DMSO-d_6) δ 1.22 (2H, m), 1.60 (4H, m), 1.75 (4H, m), 2.14 (12H, s), 2.24 (4H, t, J = 7.0 Hz), 3.18 (4H, q, J = 6.2 Hz), 3.80 (6H, s), 4.38 (4H, t, J = 7.2 Hz), 6.79 (2H, d, J = 1.7 Hz), 7.19 (2H, d, J = 1.7 Hz), 7.58 (2H, d, J = 1.7 Hz), 7.95 (2H, s), 8.12 (2H, t, J = 5.5 Hz), 8.22 (2H, d, J = 1.7 Hz), 10.23 (2H, s); FABMS m/e (relative intensity) 793 (3), 601 (2), 556 (0.7), 119 (100), 103 (62); HRFABMS m/e 793.4114 (M + H, 793.4109 calcd for $C_{37}H_{53}N_{12}O_8$).

5c: IR (powder) ν_{max} 3750–1850 (s, broad), 1652 (s), 1422 (s), 1313 (s), 1114 (m) cm^{-1}; ^{1}H-NMR (DMSO-d_6) δ 1.23 (4H, m), 1.62 (4H, t, J = 5.9 Hz), 1.70 (4H, m), 2.16 (12H, s), 2.32 (4H, t, J = 5.9 Hz), 3.18 (4H, q, J = 5.9 Hz), 3.78 (6H, s), 4.37 (4H, m), 6.80 (2H, d, J = 1.8 Hz), 7.18 (2H, d, J = 1.8 Hz), 7.57 (2H, d, J = 1.8 Hz), 8.12 (2H, t, J = 5.9 Hz), 8.19 (2H, d, J = 1.8 Hz), 10.23 (2H, s); FABMS m/e (relative intensity) 807 (1, M + H), 792 (1), 615 (2), 391 (1), 119 (100); HRFABMS m/e 807.4226 (M + H, 807.4265 calcd for $C_{38}H_{55}N_{12}O_8$).

5d: 54%; IR (powder) ν_{max} 3650–2500 (s, broad), 3127 (m), 2938 (s), 1637 (vs), 1501 (vs), 1310 (vs) cm^{-1}; ^{1}H-NMR (DMSO-d_6) δ 1.21 (6H, m), 1.63 (8H, m), 2.12 (12H, s), 2.24 (4H, t, J = 7.0 Hz), 3.16 (4H, m), 3.78 (6H, s), 4.34 (4H, t, J = 6.8 Hz), 6.79 (2H, d, J = 1.8 Hz), 7.18 (2H, d, J = 1.8 Hz), 7.54 (2H, d, J = 1.8 Hz), 8.11 (2H, t, J = 5.7 Hz), 8.19 (2H, d, J = 1.8 Hz), 10.21 (2H, s); FABMS m/e (relative intensity) 821 (11, M + H), 459 (1), 149 (53), 129 (100), 103 (74); HRFABMS m/e 821.4387 (M + H, 821.4422 calcd for $C_{39}H_{57}N_{12}O_8$).

Hexapyrroles 7a–d with Dihydrochloride Salts 1a–d. Platinum oxide (12.5 mg) was introduced to an anhydrous methanol solution (2.5 mL) of compound **5c** (50.0 mg, 0.062 mmol). Evacuation of air by the freeze and thaw procedure was followed by a charge of hydrogen. The mixture was stirred vigorously at room temperature under a 1-atm hydrogen atmosphere for 3 h. Methanol was evaporated *in vacuo*, and DMF (2.0 mL) was introduced. DMF was removed under vacuum and reintroduced (2.0 mL). To the new DMF mixture was added activated ester **6** (50.0 mg). The resulting mixture was heated at 55 °C for 4 h under nitrogen. The crude mixture was concentrated and purified from silica gel TLC with a concentrated ammonia solution and methanol (1:20, v/v). Compound **7c** was eluted from silica gel with ammonia solution and methanol (1:9, v/v). Concentration of the solution provided a yellowish solid which was dissolved in DMF. The DMF solution was centrifuged and the precipitate discarded. Evaporation of DMF resulted in a yellow solid (30.5 mg, 51% yield). Dilute hydrochloric acid solution (0.01 M) was added to the solid in a small amount of methanol at ~5 °C until the pH reached ~5, and then the solvent was evaporated. The above crude salt was dissolved in methanol and the solution precipitated with ether fractionally. The initial fractions were discarded. Concentration of the remaining fractions provided **1c** as a light yellow solid (20.0 mg, 33%).

7a: yield 46%; ^{1}H-NMR (DMSO-d_6) δ 1.69 (8H, m), 2.45 (12H, s), 2.53 (4H, t, J = 7.2 Hz), 3.19 (4H, m), 3.78 (6H, s), 3.83 (6H, s), 4.30 (4H, bs), 6.86 (2H, s), 6.90 (2H, s), 7.17 (2H, s), 7.18 (2H, s), 7.28 (2H, s), 8.09 (2H, s), 8.12 (2H, t, J = 1.5 Hz), 9.90 (2H, s), 9.92 (2H, s), 10.07 (2H, s). **1a**: yield UV (buffer, c = 7.81 μM) λ_{max} 240 nm (ϵ = 3.15 × 10^4), 300 nm (ϵ = 2.05 × 10^4); IR (powder) ν_{max} 3600–2000 (s, broad), 2961 (s), 1652 (s), 1527 (s), 1438 (s), 1257 (m) cm^{-1}; ^{1}H-NMR (DMSO-d_6) δ 1.65 (4H, m), 1.82 (4H, m), 2.70 (12H, s), 2.97 (4H, m), 3.26 (4H, m), 3.80 (6H, s), 3.83 (6H, s), 4.30 (4H, m), 4.46 (2H, bs), 6.90 (4H, bs), 7.03 (2H, s), 7.19 (2H, s), 7.30 (2H, s), 8.12 (2H, s), 8.17 (2H, m), 9.94 (4H, bs), 10.10 (2H, s), FABMS m/e (relative intensity) 1020 (0.7, M − 2HCl + H), 781 (0.1), 535 (0.5), 397 (0.9) 119 (100); HRFABMS m/e 1019.5277 (M − 2HCl + H, 1019.5327 calcd for $C_{50}H_{67}N_{16}O_8$).

7b: ^{1}H-NMR (DMSO-d_6) δ 1.24 (2H, m), 1.62 (8H, m), 2.14 (12H, s), 2.22 (4H, t, J = 7.2 Hz), 3.19 (4H, m), 3.79 (6H, s), 3.85 (6H, s), 4.28 (4H, t, J = 6.8 Hz), 6.83 (2H, d, J = 1.8 Hz), 6.93 (2H, d, J = 1.8 Hz), 7.02 (2H, d, J = 1.8 Hz), 7.18 (2H, d, J = 1.8 Hz), 7.22 (2H, d, J = 1.8 Hz), 7.30 (2H, d, J = 1.8 Hz), 8.08 (2H, t, J = 5.2 Hz), 8.13 (2H, s), 9.90 (2H, s), 9.95 (2H, s), 10.09 (2H, s). **1b**: yield 49%; (buffer, c = 7.25 μM) λ_{max} 240 nm (ϵ = 1.78 × 10^4), 300 nm (ϵ = 1.25 × 10^4); IR (powder) ν_{max} 3650–2100 (vs, broad), 2945 (vs), 1644 (vs), 1535 (s), 1263 (s) cm^{-1}; ^{1}H-NMR (DMSO-d_6) δ 1.25 (2H, m), 1.68 (4H, m), 1.84 (4H, m), 2.70 (12H, s), 3.00 (4H, m), 3.24 (4H, m), 3.80 (6H, s), 3.84 (6H, s), 4.28 (4H, bs), 4.47 (2H, bs), 6.91 (2H, s), 6.94 (2H, s), 7.03 (2H, s), 7.19 (4H, bs), 7.30 (2H, s), 8.12 (2H, s), 8.16 (2H, t, J = 1.5 Hz), 9.93 (2H, s), 9.96 (2H, s), 10.10 (2H, s); FABMS m/e (relative intensity) 1034 (0.9, M − 2HCl + H), 523 (0.8), 481 (1.2), 433 (1.3), 177 (100); HRFABMS m/e 1033.5437 (M − 2HCl + H, 1033.5484 calcd for $C_{51}H_{69}N_{16}O_8$).

7c: ^{1}H-NMR (DMSO-d_6) δ 1.22 (4H, m), 1.63 (4H, m), 1.77 (4H,

m), 2.57 (12H, s), 2.81 (4H, m), 3.22 (4H, m), 3.79 (6H, s), 3.83 (6H, s), 4.25 (4H, m), 6.87 (2H, d, J = 1.5 Hz), 6.91 (2H, d, J = 1.5 Hz), 6.99 (2H, d, J = 1.5 Hz), 7.16 (2H, d, J = 1.5 Hz), 7.18 (2H, d, J = 1.5 Hz), 7.25 (2H, d, J = 1.5 Hz), 8.12 (2H, s), 8.14 (2H, m), 9.90 (2H, s), 9.93 (2H, s), 10.09 (2H, s). **1c**: UV (buffer, c = 7.28 μM) λ_{max} 240 nm ($\epsilon = 3.02 \times 10^4$), 300 nm ($\epsilon = 2.23 \times 10^4$); IR (powder) ν_{max} 3700–1900 (s, broad), 1648 (s), 1521 (s), 1261 (m), 1130 (m) cm^{-1}; ^{1}H-NMR (DMSO-d_6) δ 1.15 (4H, m), 1.64 (4H, m), 1.80 (4H, m), 2.70 (12H, m), 2.94 (4H, m), 3.24 (4H, m), 3.81 (6H, s), 3.85 (6H, s), 4.27 (4H, m), 4.46 (2H, bs), 6.89 (2H, s), 6.91 (2H, s), 7.00 (2H, s), 7.16 (2H, s), 7.18 (2H, s), 7.25 (2H, s), 8.12 (2H, s), 8.16 (2H, m), 9.90 (2H, s), 10.08 (2H, s); FABMS m/e (relative intensity) 1084 (0.4, M – HCl + H), 1070 (0.8, M – 2HCl + Na), 1048 (1, M – 2HCl + H), 633 (0.1), 481 (3), 329 (24), 177 (100); HRFABMS m/e 1047.5592 (M – 2HCl + H, 1047.5640 calcd for $C_{52}H_{71}N_{16}O_8$).

7d: ^{1}H-NMR (DMSO-d_6) δ 1.21 (6H, m), 1.60 (8H, m), 2.12 (12H, s), 2.22 (4H, t, J = 7.2 Hz), 3.17 (4H, m), 3.79 (6H, s), 3.84 (6H, s), 4.25 (4H, t, J = 6.2 Hz), 6.80 (2H, d, J = 1.9 Hz), 6.90 (2H, d, J = 1.9 Hz), 6.99 (2H, d, J = 1.9 Hz), 7.16 (2H, d, J = 1.9 Hz), 7.19 (2H, d, J = 1.9 Hz), 7.25 (2H, d, J = 2H), 8.08 (2H, t, J = 5.0 Hz), 8.12 (2H, s), 9.87 (2H, s), 9.91 (2H, s), 10.09 (2H, s). **1d**: yield 52%; UV (buffer, c = 7.78 μM) λ_{max} 240 nm ($\epsilon = 4.37 \times 10^4$), 306 nm ($\epsilon = 4.93 \times 10^4$); IR (powder) ν_{max} 3600–2200 (s, broad), 2928 (s), 1648 (vs), 1535 (vs), 1261 (m) cm^{-1}; ^{1}H-NMR (DMSO-d_6) δ 1.24 (6H, m), 1.63 (4H, m), 1.78 (4H, m), 2.57 (12H, s), 2.78 (4H, m), 3.11 (4H, m), 3.80 (6H, s), 3.83 (6H, s), 4.27 (4H, m), 4.47 (2H, bs), 6.87 (2H, d, J = 2.0 Hz), 6.92 (2H, d, J = 2.0 Hz), 7.00 (2H, d, J = 2.0 Hz), 7.22 (2H, d, J = 2.0 Hz), 7.24 (2H, d, J = 2.0 Hz), 7.28 (2H, d, J = 2.0 Hz), 8.13 (2H, s), 8.15 (2H, t, J = 5.0 Hz), 9.90 (2H, s), 9.93 (2H, s), 10.08 (2H, s); FABMS m/e (relative intensity) 1062 (0.07, M – 2HCl + H), 857 (0.09), 627 (0.3), 179 (53), 103 (100); HRFABMS m/e 1061.5751 (M – 2HCl + H, 1061.5797 calcd for $C_{53}H_{73}N_{16}O_8$).

Monomer 8. *N*-[(Dimethylamino)propyl]-1-methyl-4-(1-methyl-4-nitropyrrole-2-carboxamido)pyrrole-2-carboxamide (100 mg, 0.266 mmol), platinum oxide (15 mg), and anhydrous methanol (3.0 mL) were mixed and evacuated by the freeze and thaw procedure to remove air. The mixture was stirred vigorously under a 1-atm hydrogen atmosphere at room temperature for 2 h. Methanol was then evaporated *in vacuo* and DMF (3.0 mL) introduced. After addition of the activated ester **6** (100 mg, 0.302 mmol), the mixture was heated at 55 °C for 4 h under argon. The crude mixture was concentrated and eluted with concentrated ammonia solution and methanol (1:20, v/v) on a silica gel TLC plate. The corresponding amine of monomer **8** was washed from the silica gel with a concentrated ammonia solution and methanol mixture (1:9, v/v). Concentration of the collected solution gave a yellow solid which was redissolved in a small amount of methanol (5 mL). This methanol mixture was centrifuged. The silica gel precipitate was discarded, and the supernatant was concentrated in vacuo to afford a yellow solid (106 mg). The amine dissolved in a small amount of methanol was neutralized with dilute hydrochloric acid (0.05 M) at 5 °C. Evaporation *in vacuo* furnished the ammonium salt **8** as a yellow solid (110 mg, 78%): UV (buffer, c = 9.00 μM) λ_{max} 240 nm ($\epsilon = 1.75 \times 10^4$), 300 nm ($\epsilon = 7.74 \times 10^3$); IR (powder) ν_{max} 3650–2500 (s, broad), 3125 (m), 2945 (s), 1637 (vs), 1526 (vs), 1258 (s) cm^{-1}. ^{1}H-NMR (DMSO-d_6) δ 1.67 (2H, m), 2.29 (6H, s), 2.43 (2H, m), 3.21 (q, J = 6.0 Hz), 3.71 (3H, s), 3.75 (6H, s), 6.83 (1H, d, J = 1.9 Hz), 6.91 (1H, d, J = 1.9 Hz), 7.02 (1H, d, J = 1.9 Hz), 7.17 (1H, d, J = 1.9 Hz), 7.19 (1H, d, J = 1.9 Hz), 7.22 (1H, d, J = 1.9 Hz), 8.09 (1H, t, J = 6.0 Hz), 8.11 (1H, s), 9.90 (1H, s), 9.93 (1H, s), 10.09 (1H, s); EIMS m/e (relative intensity) 496.2537 (2, M – HCl, 496.2546 calcd for $C_{24}H_{32}N_8O_4$), 468 (2), 273 (7), 151 (17), 123 (12), 58 (100).

Activated Ester 6. To ester **9** (1.00 g, 5.49 mmol) in anhydrous methanol (10.0 mL) was added 10% palladium on charcoal (100 mg). The air was evacuated and hydrogen charged. The mixture was stirred vigorously at room temperature for 3 h. Sodium hydroxide solution (2 M, 7.5 mL) was introduced, and the mixture was introduced, and the mixture was stirred over 6 h under nitrogen and then cooled to 0 °C. Formic acetic anhydride in ether (7.3 M, 3.0 mL) was added. The reaction mixture was warmed to room temperature, then stirred for additional 30 min and filtered. Acidification with hydrochloric acid (6 M) to pH = 4 gave acid **10** as a white solid precipitate (0.71 g). The acid was dissolved in anhydrous DMF (10 mL), HOOBt (0.75 g) and EDCI (0.90 g) were introduced, and the mixture was stirred for 1 h. The reaction mixture was diluted with dichloromethane (40 mL) and then extracted with water. Concentration of the organic layer afforded a yellow solid which was chromatographed with acetone and dichloromethane (1:4, v/v). The activated ester **6** was obtained as a yellow solid (0.88 g, 67% yield): mp 197–199 °C (decomposed); IR (powder) ν_{max} 3350 (s), 1756 (s), 1713 (s), 1440 (m), 1182 (m); ^{1}H-NMR ($CDCl_3$) δ 3.93 (3H, s), 7.13 (1H, d, J = 1.8 Hz), 7.40 (1H, bs), 7.69 (1H, d, J = 1.8 Hz), 7.88 (1H, td, J = 8.0 and 0.9 Hz), 8.04 (1H, td, J = 8.0 and 1.5 Hz), 8.27 (1H, dd, J = 8.0 and 0.9 Hz), 8.32 (1H, d, J = 1.6 Hz), 8.42 (1H, dd, J = 8.0 and 1.5 Hz); EIMS m/e (relative intensity) 313.0807 (5, 313.0811 calcd for $C_{14}H_{11}N_5O_4$), 216 (2), 168 (15), 151 (100), 140 (7). Anal. Calcd for $C_{14}H_{11}N_5O_4$: C, 53.67; H, 3.54; N, 22.36. Found: C, 53.82; H, 3.37; N, 22.20.

Acknowledgment. Professor R. S. Brown kindly permitted the use of the Inplot 4.01 program in his group, and Dr. O. Nunez offered helpful assistance in utilizing the program. Mr. A. Guo gave valuable advices on using the KaleidaGraph 2.1 software. Discussion on ethidium bromide fluorescence displacement experiments with Professor A. R. Morgan in the Department of Biochemistry at the University of Alberta was very enlightening and stimulating. We thank the Natural Sciences and Engineering Research Council of Canada for financial support (to J.W.L.) of this research program. Y.-H.C. expresses his sincere thanks to Professor William von Egger Doering of Harvard University for initiating the chemistry Graduate Program with the P. R. China. Y.-H. C. was accepted to this program at the University of British Columbia in 1986.